



Identification of Promising Inhibitors from Natural Compounds Targeting PlmX, a Multi-Stage Drug Target in Plasmodium Falciparum

Cheickna CISSE^{*1}, Oudou DIABATE¹, Mamadou WELE¹, Mamadou SANGARE¹, Alia BENKAHLA², Jeffrey SHAFFER³, Seydou DOUMBIA⁴

Abstract

The emergence of resistance to the first-line antimalarial drugs poses a significant threat to recent progress in the fight against malaria. It is imperative to discover novel therapeutic drugs for Malaria. Utilizing rational methods facilitated by bioinformatics tools presents the most efficient and cost-effective approach to achieve this imperative. The objective of this study was: first, to model an active structure of Plasmepsin X (PlmX) a potent multistage drug target from *Plasmodium falciparum*, and second, to identify potential inhibitors from African databases of Natural Products. The model was constructed utilizing a multiple templates approach implemented in Modeller. The best model obtained underwent validation using standard tools. Subsequently, a high throughput virtual screening was conducted using Autodock Vina, employing African databases of Natural Products. The results demonstrated the successful construction of an accurate and validated model of PlmX. A total of 8690 compounds sourced from natural active compounds were screened, leading to the identification of 68 compounds exhibiting high affinity (docking score ≤ -9 kcal/mol). Further analysis revealed detailed interactions of top ten promising inhibitors, highlighting their potential as effective inhibitors. This study identified promising inhibitors to be considered in the development of new and effective antimalarial drugs.

Keywords: *Plasmodium falciparum* malaria, protein modeling, virtual screening, Natural Compounds inhibitors

Introduction

Malaria represents a significant global health challenge, with an estimated 249 million cases of Malaria and 608 thousand malaria-related deaths reported worldwide in 2023. disproportionately borne by pregnant women and children under 5 years of age [1]. Notably, this burden was an increase of about 5 million cases in 2022 compared to 2021. African countries carry the heaviest burden, accounting for about 233 million cases, which make up 94% of all malaria cases, and 94% of malaria-related deaths in 2022 [1]. Despite recent significant advances in the fight against malaria, it remains a persistent public health problem due to the emergence of parasite resistance to antimalarial drugs and of Anopheles mosquitoes to insecticides [1]. Indeed, Artemisinin and its derivatives, which serve as the last line of defense in antimalarial treatment, have lost their effectiveness in the Asian continent [2] due to parasite resistance. The potential spread of this multidrug-resistant

Affiliation:

¹African Centre of Excellence in Bioinformatics (ACE-B), USTTB, Bamako, Mali

²Institute Pasteur of Tunis, Tunisia

³School of Public Health and Tropical medicine, New-Orleans, Louisiana, USA

⁴University of clinical Research Center (UCRC), USTTB, Bamako, Mali

*Corresponding author:

Cheickna CISSE, African Centre of Excellence in Bioinformatics (ACE-B), USTTB, Bamako, Mali.

Citation: Cheickna CISSE, Oudou DIABATE, Mamadou WELE, Mamadou SANGARE, Alia BENKAHLA, Jeffrey SHAFFER, Seydou DOUMBIA, Mamadou WELE. Identification of Promising Inhibitors from Natural Compounds Targeting PlmX, a Multi-Stage Drug Target in Plasmodium Falciparum. Journal of Pharmacy and Pharmacology Research. 8 (2024): 55-65.

Received: July 06, 2024

Accepted: July 15, 2024

Published: October 29, 2024

P. falciparum to the African continent is a cause for concern, as has happened in the past. Therefore, the pressing need lies in the discovery of novel and effective antimalarial targets. This requires the identification and validation of new drug targets within malaria parasites and their structural characterization. This is particularly pertinent for *P. falciparum*, the most prevalent malaria species in humans, responsible for 80% of all malaria infections and severe complications leading to death [3].

Numerous studies have extensively investigated *P. falciparum*, generating valuable insights data on its genome and metabolic pathways [4], [5], [6], [7]. Leveraging data from these studies, bioinformatics tools have been developed to predict potential drug targets against pathogens. Notably, the World Health Organization's Special Program for Research and Training in Tropical Diseases has developed the TDR Targets server [8]. A key function of this server is conducting genomic-scale analyses of pathogens, categorizing, and prioritizing multiple proteins as potential drug candidates based on user-defined criteria [9]. The criteria for potential drug targets rely on their essential roles in the pathogen's survival and their lack of orthology in Human hosts [10]. Identifying drug targets has become more feasible through well-established criteria. Numerous studies have predicted promising malaria drug targets [5], [6], [7], [10], [11], [12], [13]. The new challenge lies in the structural characterization of these targets facilitates the design structure-based inhibitors [14]. Recently, several tools and databases have been developed to overcome this problem [15], [16]. One of these methods is homology modeling [15], [17], used in this study. This method is used if the 3D structure of the target is not available. So, the method uses a template-based modeling to predict a 3D structure which must be assessed and validated for further studies [18]. Once a valuable 3D model is available, a structure-based virtual screening using a bank of molecules is conducted to determine potential inhibitors. Many works have confirmed that the PlmX from *Plasmodium falciparum* is an antimalarial target [19], [20], [21]. To date, the global active structure of the protein is not available yet. In this study, the 3D model was built based on multiple templates approach combining different modeling tools. The African continent abounds in natural resources, particularly medicinal substances [22]. To find potential inhibitors available and accessible on the continent, virtual screening with diverse natural products sourced from African databases AfroDb [23], EANPDB [24], NANPDB [25] and SANCDB [26], [27]. Different analyses were undertaken to determine the most promising inhibitors and they interactions with the targets. Those with the best pharmacological properties for the development of new and effective antimalarial candidates were selected for biological assessments.

Materials and Methods

Target Sequence Alignment

A first alignment with BLASTp [28] were performed with PlmX from *Plasmodium falciparum* (Code UniProt: Q8IAS0) to identify homologous proteins. The default parameters were used with the database set to Protein Data Bank [29]. This research identified the crystallographic structures of PlmX (Code PDB: 6ORS, 7RY7, 7TBB, 7TBC, 8DSR). All the structures were missing some segments of the entire sequence. To get the complete 3D structure of the protein for valuable docking a new model was built.

Homology modeling and Refinement

After comparison of the structures *via* Chimera (Supplementary data, **Figure 5**) the PDB coordinates code 7TBB with a resolution of 1.85 Å were selected, the missing residues were built with Model/Refine Loops module of Modeller using the AlphaFold model AF-Q8IAS0-F1 of PlmX. Among the initial models generated during this process, the one with the least DOPE score energy value and the least deviation from PDB structure was considered as the PfPlmX model for further investigation. The selected model was refined by a molecular simulation optimization protocol using NAMD 2.9 [30] on a quad core Intel® Core™ i7-4600 CPU 2.90 GHz processor. The CHARMM 27 force field [31] was used for energy minimization and the simulation was carried out in the Visual Molecular Dynamics (VMD) tool [32]. The system was minimized during 25 000 steps and the refined model was used. The process was repeated three times.

Validation of the 3D model

The quality of the simulated model was assessed by ProSA-web: interactive web service for the recognition of errors in three-dimensional structures of proteins the stereo chemical [33], and on the structure validation server SAVES (<https://saves.mbi.ucla.edu/>). ERRAT which is a program for verifying protein structures determined by crystallography [34] and VERIFY 3D [35], [36] and PROCHECK [37] were used to assess the quality of the models. MolProbity is a structure validation web service for diagnosing problems in 3D models of proteins [38] was also used to check errors.

Prediction of binding pockets:

The Computed Atlas of Surface Topography of proteins (CASTp) [39] was used to calculate the ligand binding pockets of the protein. The pockets with the biggest volume area covering the native active binding site were chosen to define the maximum grid box for the virtual screening.

Protein preparation:

The protein was prepared with the graphical interface

AutoDockTool-1.5.7 (ADT) [40]. The protocol included removal of non-polar Hydrogens, adding of the Gasteiger charges, and assigning solvation parameters and Atom Types. ADT was used to define the grid box coordinates set to center x, y and z equal 22.992, 28.473 and 26.236 resp.; the npts x, y and z = 66, 84, and 78 resp.; and grip spacing = 0.375. The box was defined large enough to cover the three best binding pockets calculated by CASTp and to accommodate complex ligand structures usually found in NPs.

Ligand preparation for structure-based virtual screening:

The ligands were selected from the following African databases of NPs: AfroDb, EANPDB, NANPDB and SANCDB. A total of 8741 molecules found through these databases were converted to .pdb formats using PyRx [41] and Open Babel [42] using homemade scripts. Then the compounds were prepared using ADT which added Gasteiger charges, Atom Types parameter and defined rotatable bonds and finally converted the files to .pdbqt formats for virtual screening. The compound 49c and WM382 known as potent inhibitor of PlmX [19], [20] was also prepared using the same protocol and was used as control for comparative analysis.

Virtual screening of PlmX

The widely docking program AutoDock Vina v.1.2.0 [43], known for its accuracy, high speed performance and reliability, for structure-based virtual screening was used to search and calculate docking poses of the ligands on the protein. The protocol was carried out as following: the validated 3D model of PlmX was used as receptor, the ligand was the list of NPs, the grid box previously calculated by ADT was used, the exhaustiveness value = 8 was used and 9 conformations were generated per ligand. The screening was

launched on the server of the Mali International Center for Excellence in Research (ICER).

Docking analysis

The results of virtual screening were analyzed by the following visualization programs: ADT, Pymol-2.0 [44], [45] and UCSF Chimera [46]. The ligands with high affinity (Score ≤ -9 Kcal/mol) were considered for attentive examination. Those fitting well into the active site were considered as the most promising inhibitors and for identifying interactions details with the Ligplot+ v.2.2.4 software.

Results

3D structure of active PlmX

To operate a structure-based screening, it is important to consider the most accurate as possible 3D structure. As the PDB coordinates of PlmX (code PDB: 6ORS) were missing the following segments: M1---R28, K69---D73, L130---N225, E304---S315, E343---D352, we carried out a multiple templates modeling with Modeler using the AlphaFold model of PlmX (AFv1-Q8IAS0) as another template. The best model among the hundreds of models generated by Modeler with the lowest DOPE score -56547.92 and GA341 of 1.00 was selected. To perform the docking consistently with the native conditions [19], [48], the segment K69---S246 covering the active site was deleted. The new numbering was comprised between ARG1 to ASN439. The molecular dynamics simulation operated on the new model showed energy stability which moved from 199921.90 to -33140.35 KJ/mol. The conformation with the lowest energy was displayed on Figure 1. Like other members of Aspartate Protease family, the model showed the N-terminal and C-terminal domain linked by pseudo twisted β -barrel [19], [48], [49].

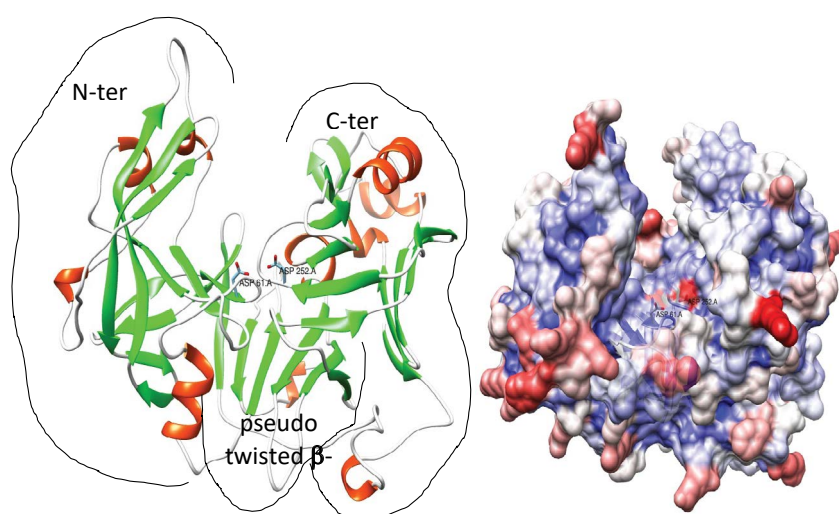


Figure 1: 3D-Model of active PlmX. Left: Cartoon representation of protein backbone with Beta-sheets in green and Alpha-Helices in brown, the catalytic aspartates ASP61 and ASP 252 are shown in licorice, cyan. The three domains (N-ter, C-ter and pseudo twisted) are surrounded by dashed lines. Right: Surface representation of protein showing the binding pocket above the catalytic aspartates.

3D model validation

The quality of the 3D model of PlmX were analyzed by five of the structure validation tools: VERIFY-3D, ERRAT, ProSA, PROCHECK and MolProbity. **Table 1** summarizes the results obtained.

Table 1: Quality control values of 3D model

ProSA	ERRAT	VERIFY 3D	PROCHECK		MolProbity
Z-Score	Quality Factor	averaged 3D-1D score >= 0.2	favoured	allowed	Score
-8.47	92.816	91.30%	91.20%	8.20%	1.95

The values of ProSA-Web (Z-score = -9.66), ERRAT (quality factor = 92.816) and VERIFY 3D (averaged 3D-1D score = 91.30), clearly demonstrated that the overall structure of the PlmX model was very good and valuable for further investigations. In addition, PROCHECK values showed that more than 99% of the residues were in favored and allowed regions of the Ramachandran plot (supplementary info: **Figure 6**). Together these results suggested the reliability of the model for structure-based docking.

Active binding site prediction

The binding pockets were calculated by CASTp webserver [31]. The **Figure 2** showed the three potential binding pockets displayed in red volume. The pocket 1 with the largest surface area (814.36\AA^2) and a volume of 1071.627\AA^3 , predicted as the best binding pocket was covering the catalytic Aspartates and other residues of the active site. This pocket was found between the two Nter and Cter domains in accordance with the active sites of other Aspartate proteases [48], [49]. The three pockets were subsequently used for building the grid box where ligand conformations search is performed during virtual screening (**Figure 2**). The size of the grid box was set large enough to cover the three pockets to allow sufficient conformation search for NPs.

Virtual screening

The virtual screening was carried out with a library set of 8690 Natural Products from four African databases: AfroDb (<http://african-compounds.org/about/afrodb/>) [41], NANPDB (<http://african-compounds.org/nanpdb/>) [39], SANCDB (<https://sancdb.rubi.ru.ac.za/>) [37], EANPDB (<http://african-compounds.org>) [40]. The **Table II** resumed the distribution among the different databases.

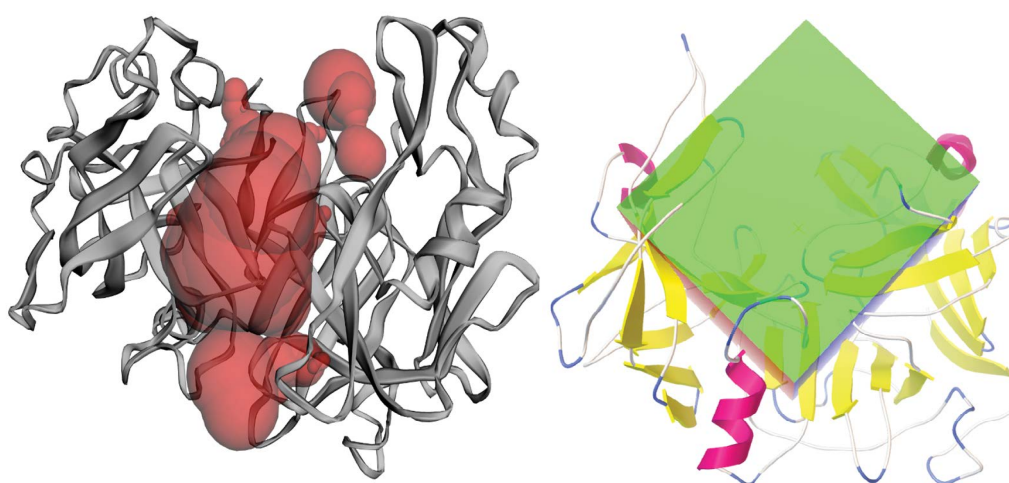


Figure 2: 3D-model of active PlmX, Left: cartoon representation of backbone with binding pockets in Red spheres predicted and Right: Grid box computed by ADT and used for virtual screening (box with green, blue and red faces) containing the binding pockets.

Table II: Distribution of molecules used for virtual screening according to their affinity for PlmX

Databases	SANCDB	NANPDB	EANPDB	AfroDb	Total
Number of Compounds	1012	4928	1870	880	8690
Number of compounds with score ≤ -8 Kcal/mol	232	1069	558	230	2089
Number of compounds with score ≤ -10 Kcal/mol	16	26	25	11	78
References	[37][38]	[39]	[40]	[41]	

In this study, all the ligands with docking score ≤ -8 Kcal/mol, total number = 2089 were considered because the inhibitors used as controls scored around this docking score value. The number of selected compounds for each database was 232, 1069, 558 and 230 for SANCDB, NANPDB, EANPDB and AfroDb respectively (**Table II**). Among them, the compounds with docking score ≤ -10 Kcal/mol (total number = 78) showing high affinity with the target were attentively examined with their nine docked poses. Their ADME properties were analyzed by SwissADME.

The best compounds with no violation of Lipinski's rule were selected for further analysis (**Table III**). Two known inhibitors of PlmX: compounds 49c (PubChem:71521073) and WM382 (PubChem:154699453) were docked with the same conditions. The compounds asphodelin, SANC00584 and SANC00585 with Mw=506.46, 510.58 and 510.58 respectively were also selected as their Mw were close to the inhibitors: 504.6 and 514.7 g/mol respectively for WM382 and compounds 49c.

Table III: List of top ten potential inhibitors of PlmX with Docking score and pharmacological parameters

#	Molecule	Formula	PubChem ID	Mw (g/mol)	H-bond acceptors	H-bond donors	MLOGP	Lipinski violations	Leadlikeness violations	Docking Score (Kcal/mol)
	EANPDB									
1	calopogonium	C ₂₁ H ₁₈ O ₄	354119	334.37	4	0	2.42	0	1	-10
2	norisojamicin	C ₂₁ H ₁₆ O ₆	101938912	364.35	6	1	1.72	0	2	-10.1
3	millettone	C ₂₂ H ₁₈ O ₆	442810	378.37	6	0	2.12	0	2	-10.2
4	millettosine	C ₂₂ H ₁₈ O ₇	15560542	394.37	7	1	1.32	0	1	-10.3
5	bianthracene III	C ₃₀ H ₂₀ O ₇	None	492.48	7	4	1.78	0	2	-10.4
6	asphodelin	C ₃₀ H ₁₈ O ₈	182665	506.46	8	4	0.92	1	2	-10.3
	AfroDb									
7	WA_0038	C ₂₀ H ₃₂ O ₂	162910809	304.47	2	2	4.07	0	1	-10.7
8	EA_0132	C ₂₉ H ₃₂ O ₄	10049125	444.56	4	1	4.12	0	2	-10.3
	SANCDB									
9	SANC00584	C ₃₂ H ₃₀ O ₆	16115666	510.58	6	2	2.62	1	2	-10.4
10	SANC00585	C ₃₂ H ₃₀ O ₆	16115802	510.58	6	2	2.62	1	2	-10.4
	Known Inhibitors									
	WM382	C ₂₉ H ₃₆ N ₄ O ₄	154699453	504.6	5	2	3.4	1	1	-8.9
	Compound 49c	C ₃₁ H ₃₈ N ₄ O ₃	71521073	514.7	5	3	3.3	1	2	-10.3

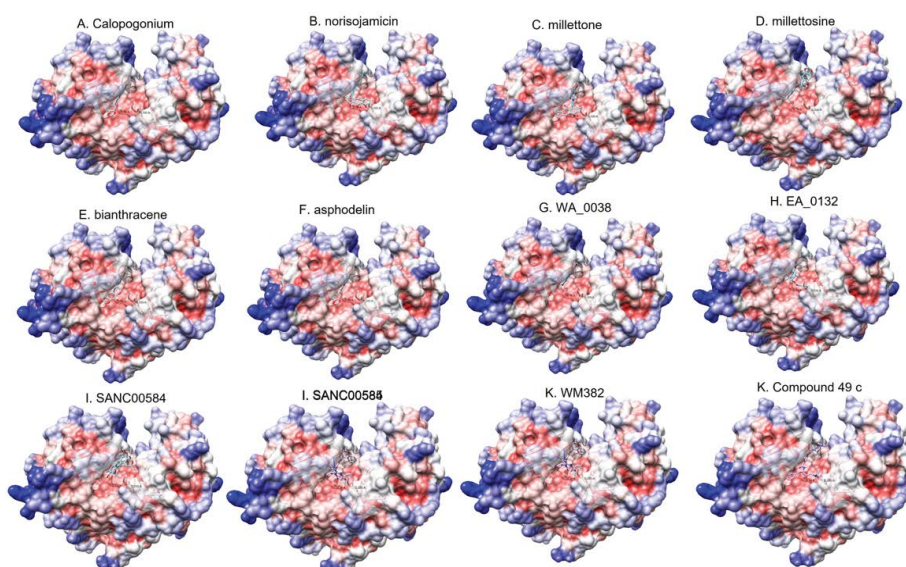


Figure 3: Best docking poses of Top ten potential inhibitors of PLMX. All the ligands are inside the cleft of the binding pocket interacting with residues surrounding the catalytic residues Asp34 and Asp220.

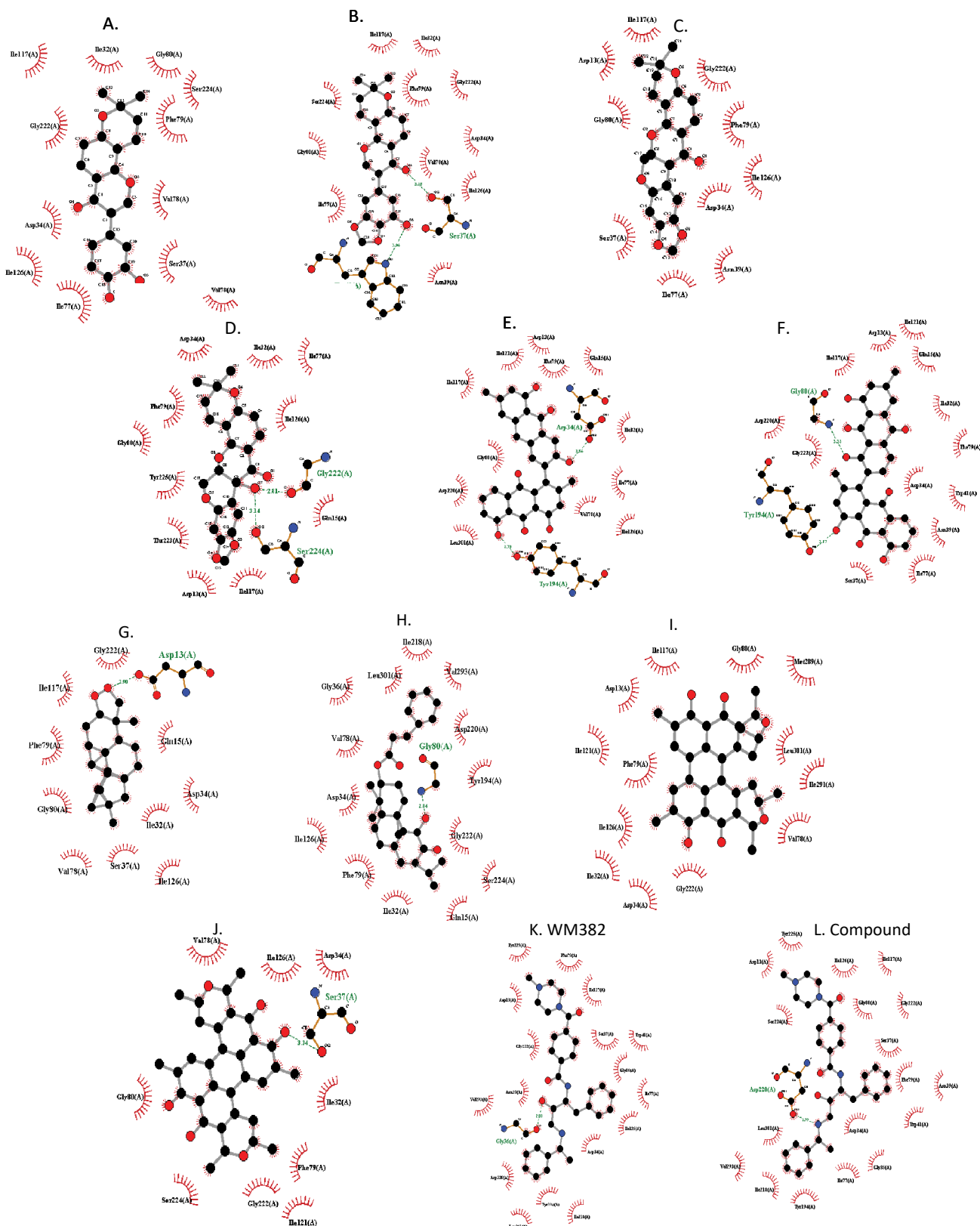


Figure 4: 2D interactions map generated by LigPlot+ program between PfPLMX and the top ten compounds (Table III). The map showed Important interactions between the ligands (Bonds colored in Gray) and the surrounding residues of the protein: Hydrogen bonds are shown by dashed (green) lines, Hydrophobic contacts between protein and ligand are indicated by the (brick-red) spoked arcs.

The selected compounds selected as potential inhibitors of PlmX showed remarkably high affinity with their target with scores ranging from -10.00 to -10.7 Kcal/mol. In comparison, standard inhibitors used as controls displayed affinity scores of -10.3 kcal/mol for **WM382** and -8.9 kcal/mol for compound **49c** (**Table III**). This indicated that the selected ligands and the inhibitors exhibited comparable affinity scores. The binding poses of the top predicted ligands were shown in **Figure 3**. As expected, all the ligands are located within the cleft of the binding pocket, interacting closely with the catalytic residues.

Interactions analyses

Figure 4 displayed interactions details between the protein

and the potential inhibitors, highlighting key Hydrogen bonds and numerous hydrophobic contacts between the protein and ligands. To comprehensively understand these interactions, a thorough analysis was conducted, the results of which are summarized in **Table IV**. This analysis revealed that the ligands bind to the protein through numerous hydrophobic interactions and hydrogen bonds. Only two ligands, Millettone and SANC00584, did not form any hydrogen bonds upon binding. The protein residues primarily involved in ligand interactions were PHE79 and ASP34, 9 times for the 10 ligands (9/10), followed by ILE117 and ILE126 (8/10), then GLY222 (7/10) and finally ILE77, GLY80, VAL78 (**Table IV**).

Table IV. Details of interactions between the target protein and potential inhibitors

Compounds	Number of H Bonds	Protein Residues involved in	
		H Bonds	VdW interactions
Calopogonium	2	ASN-39, SER-33	ILE32, GLY80, SER224, PHE79, VAL78, SER37, ILE77, ILE126, ASP34, GLY222, ILE117
Norisojamicin	3	SER-37, ASN-39,	ILE77, GLY80, SER224, ILE117, ILE32, PHE79, GLY222, ASP34, VAL78, ILE126, ASN39
		TRP-41	
Millettone	0	--	SER37, GLY80, ASP13, ILE117, GLY222, PHE79, ILE126, ASP34, ASN39, ILE77
Millettosine	2	SER224, GLY222	ILE117, GLY80, TYR225, THR223, ILE32, VAL78, ILE77, PHE79, ASP34, GLY15, ILE126, ASN39
Bianthrane	2	TYR194, ASP34	LEU301, ASP220, GLY80, ILE117, ILE121, ASP13, PHE79, GLN15, ILE32, ILE77, VAL78, ILE126
Asphodelin	2	TYR194, GLY80	GLY222, ASP220, ILE117, ASP13, ILE121, GLN15, ILE32, PHE79, ASP34, TRP42, ASN39, ILE77, SER37
WA_0038	1	ASP13	GLY80, PHE79, ILE117, GLY222, GLN15, ASP34, ILE32, ILE126, SER37, VAL78
EA_0132	1	GLY80	ILE32, PHE79, ILE126, ASP34, VAL78, GLY36, LEU301, ILE218, VAL293, ASP220, TYR194, GLY222, SER224, GLN15
SANC00584	0	--	GLY222, ASP34, ILE32, ILE126, PHE79, ILE121, ASP13, ILE117, GLY80, MET89, LEU301, ILE391, VAL78
SANC00585	1	SER37	SER224, GLY80, VAL78, ILE126, ASP34, ILE32, PHE79, GLY222, ILE121

Discussion

Considering the ongoing threat of malaria resistance, identification of new malaria drug targets and therapeutic compounds are still relevant and important. To achieve this goal efficiently and cost-effectively, computational methods and tools offer the least time-consuming and most cost-reducing means to reach this goal [50], [51]. This work highlighted how computational tools could be employed to logically design therapeutic candidates of both target and inhibitors. The rational investigation to find therapeutic

targets from the genome of *P. falciparum* conducted by TDR Target revealed a set of promising drug targets among which (unpublished) PlmX was singled out for structure-based inhibitors research. PlmX is an essential aspartyl protease, crucial for parasite egress and erythrocytes invasion making it a multiple stage drug target of the malaria lifecycle. Many recent studies have proved that PlmX is a valuable target [21], [49], [52], [53], [54]. It is known that inactivation of PlmX led to clearance of blood-stage *P. falciparum* [21], [48], [49]. In this study, a new and complete model of PlmX was built from

the crystallized structure (PDB: 6ORS) by incorporating the missing sequence: M1---R28, K69---D73, L130---N225, E304---S315, E343---D352. The model was evaluated with common methods of Protein model quality assessment: ProSA-Web values (Z-score -9.66), ERRAT (Quality factor 92.816) and VERIFY 3D (averaged 3D-1D score of 91.30). The results clearly indicated the excellent overall quality of the model **Figure 1**, confirming its suitability for structure-based inhibitors investigations. In addition, PROCHECK assessment demonstrated that over 99% of the residues were within the favored and allowed regions of the Ramachandran plot (see supplementary info: **Figure 3**). From the virtual screening analysis, ten (10) compounds were chosen as the most promising inhibitors for PlmX (**Table III**). The selected ligands exhibited comparable affinity scores like the validated inhibitors used as controls (~ -10 kcal/mol) demonstrating their remarkably high affinity with the target. The drug-likeness and pharmacokinetic properties were computed. The number of hydrogen bond acceptors (HBA, ≤10) and donors (HBD, ≤5) for all the compounds were in accordance with the Lipinski's rule of five (**Table III**). The lipophilicity (MLogP) predicted for all the compounds were found to be well for drug design. Selected compounds, except for asphodelin, SANC00584 and SANC00585 (Mw=506.46, 510.58 and 510.58 resp.), showed suitable MW values (MW < 500). This is essential for a successful penetration through biological membranes. In addition, all compounds fell into the appropriate range indicating good bioavailability of the candidate molecule. Together, these values indicate that the selected compounds displayed good drug-likeness and pharmacological properties. This suggests that these compounds represent good candidates for the development of new and effective antimalarial drugs. The details of interactions between the selected compounds and the target showed that those molecules bind to the protein through numerous hydrophobic interactions and hydrogen bonds (Figure 4, Table IV). The protein residues primarily involved in the VdW interactions are PHE79 and ASP34, followed by ILE117 and ILE126, then GLY222 and finally ILE77, GLY80, VAL78 by priority order (Table IV). The residues ASN39, SER37, TRP41, SER224, GLY222, TYR194, ASP34; GLY80, ASP13 were found to be involved in the hydrogen bonding with the compounds. Those residues have been cited by [19], [20], [48] among those involved in the interactions of mature form of PlmX in complex with a substrate and 49c, reported to inhibit PlmX. Molecular dynamics simulations and biological assays will be required to validate the stability of these interactions and confirm the effectiveness of these compounds.

Conclusion

This work has highlighted how computational tools have been used to rationally design therapeutic candidates.

The plasmepsin X from *Plasmodium falciparum* PlmX was selected from a set of malarial therapeutic targets for further structure-based inhibitor research. As the complete structure of the active form was not available, a robust 3D model was built through combinations of modeling tools and a virtual screening of Natural Products from African Databases allowed to identify promising inhibitors and they interactions modes.

Acknowledgements

We acknowledge the African Center of Excellence in Bioinformatics of Bamako (ACE-B)/USTTB for conducting and monitoring the project and the University of Clinical Research Center (UCRC)/USTTB, Mali for the technical support, the Department of Biostatistics and Data Science/ Tulane University and the Institute Pasteur of Tunis for manuscript review.

Funding

NIH Cooperative Agreements U2R TW010673 supported this study for West African Center of Excellence for Global Health Bioinformatics Research Training. The study team members received financial support from H3ABioNet (U24HG006941).

Disclosure Statement

The authors report there are no competing interests to declare

References

1. W. Health Organization, World malaria report 2022 (2023).
2. S. Takala-Harrison and M. K. Laufer, "Antimalarial drug resistance in Africa: Key lessons for the future," *Ann N Y Acad Sci* 1342 (2015): 62–67.
3. FS Buckner, NC Waters, and VM Avery, "Recent highlights in anti-protozoan drug development and resistance research," *Int J Parasitol Drugs Drug Resist* 2 (2012): 230–235.
4. M. Mishra, V. Singh, and S. Singh, "Structural Insights Into Key Plasmodium Proteases as Therapeutic Drug Targets," *Front Microbiol* 10 (2019): 394.
5. R G Ducati, HA Namanja-Magliano and VL Schramm, "Prospective Enzyme Targets in Malaria," *Future Med. Chem* 5 (2013): 1341–1360.
6. N. Dholakia, P. Dhandhukia, and N. Roy, "Screening of potential targets in *Plasmodium falciparum* using stage-specific metabolic network analysis," *Mol Divers* (2015).
7. A. K. Banerjee, N. Arora, and U. S. N. Murty, "Structural model of the *Plasmodium falciparum* thioredoxin

- reductase: a novel target for antimalarial drugs.,” *J Vector Borne Dis* 46 (2009): 171–183.
8. L. Urán Landaburu et al., “TDR Targets 6: driving drug discovery for human pathogens through intensive chemogenomic data integration,” *Nucleic Acids Res*, vol. 48, no. D1, pp. D992–D1005, Nov. (2019).
 9. F. Agüero et al., “Genomic-scale prioritization of drug targets: the TDR Targets database,” *Nat Rev Drug Discov* 7 (2008): 900.
 10. QF. He, D. Li, Q. Y. Xu, and S. Zheng, “Predicted essential proteins of *Plasmodium falciparum* for potential drug targets,” *Asian Pac J Trop Med* 5 (2012): 352–354.
 11. S. Y. Bah, C. M. Morang’a, J. A. Kengne-Ouafo, L. Amenga-Etego, and G. A. Awandare, “Highlights on the Application of Genomics and Bioinformatics in the Fight Against Infectious Diseases: Challenges and Opportunities in Africa,” *Front Genet* 9 (2018): 575.
 12. G. J. Crowther et al., “Identification of attractive drug targets in neglected- disease pathogens using an in Silico approach,” *PLoS Negl Trop Dis* 4 (2010): 8.
 13. C. L. Ng, D. A. Fidock, and M. Bogyo, “Protein Degradation Systems as Antimalarial Therapeutic Targets,” *Trends Parasitol* 33 (2017): 731–743.
 14. S. Z. Grinter and X. Zou, “Challenges, applications, and recent advances of protein-ligand docking in structure-based drug design,” *Molecules* 19 (2014): 10150–10176.
 15. L. G. Ferreira, R. N. Dos Santos, G. Oliva, and A. D. Andricopulo, “Molecular docking and structure-based drug design strategies,” vol. 20, no. 7. 2015. doi: 10.3390/molecules200713384.
 16. B. L. Staker, G. W. Buchko, and P. J. Myler, “Recent contributions of structure-based drug design to the development of antibacterial compounds,” *Curr Opin Microbiol* 27 (2015): 133–138.
 17. I. Kufareva and R. Abagyan, “Homology Modeling Exercise,” *Methods Mol Biol* 857 (2012): 231–257.
 18. R. Adiyaman and L. J. McGuffin, “Methods for the refinement of protein structure 3D models,” *Int J Mol Sci* 20 (2019).
 19. G. Munsamy, P. Ramharack, and M. E. S. Soliman, “Egress and invasion machinery of malaria: An in-depth look into the structural and functional features of the flap dynamics of plasmepsin IX and X,” *RSC Adv* 8 (2018).
 20. G. Munsamy, C. Agoni, and M. E. S. Soliman, “A dual target of Plasmepsin IX and X: Unveiling the atomistic superiority of a core chemical scaffold in malaria therapy,” *J Cell Biochem* 120 (2019).
 21. P. Favuzza et al., “Dual Plasmepsin-Targeting Antimalarial Agents Disrupt Multiple Stages of the Malaria Parasite Life Cycle,” *Cell Host Microbe* 27 (2020).
 22. A. K. Mamadou et al., “Evaluation of the biological activities of leaf and bark extracts of *Ficus platiphylla* Delile, a medicinal plant used in Mali,” *Journal of Medicinal Plants Research* 14 (2020): 118–128.
 23. F. Ntie-Kang et al., “AfroDb: a select highly potent and diverse natural product library from African medicinal plants,” *PLoS One* 8 (2013): 1–15.
 24. C. V. Simoben et al., “Pharmacoinformatic Investigation of Medicinal Plants from East Africa,” *Mol Inform* 39 (2020): 1–15.
 25. F. Ntie-Kang et al., “NANPDB: A Resource for Natural Products from Northern African Sources,” *J Nat Prod* 80 (2017): 2067–2076.
 26. R. Hatherley et al., “SANCDB: a South African natural compound database,” *J Cheminform* 7 (2015): 29.
 27. B. N. Diallo, M. Glenister, T. M. Musyoka, K. Lobb, and Ö. Tastan Bishop, “SANCDB: an update on South African natural compounds and their readily available analogs,” *J Cheminform* 13(2021): 1–14.
 28. S. F. Altschul, W. Gish, W. Miller, E. W. Myers, and D. J. Lipman, “Basic local alignment search tool,” *J Mol Biol* 215 (1990): 403–410.
 29. H. M. Berman et al., “The Protein Data Bank,” *Nucleic Acids Res* 28 (2000): 235–242.
 30. J. C. Phillips et al., “Scalable molecular dynamics with NAMD,” *J Comput Chem* 26 (2005): 1781–1802.
 31. B. R. Brooks, R. E. Bruccoleri, B. D. Olafson, D. J. States, S. Swaminathan, and M. Karplus, “CHARMM: The Biomolecular Simulation Program,” *J Comput Chem* 30 (2010): 1545–1614.
 32. W. Humphrey, A. Dalke, and K. Schulten, “VMD: visual molecular dynamics,” *J Mol Graph* 14 (1996): 27–28.
 33. M. Wiederstein and M. J. Sippl, “ProSA-web: interactive web service for the recognition of errors in three-dimensional structures of proteins,” *Nucleic Acids Res*, vol. 35, no. Web Server issue (2007): W407–10.
 34. C. Colovos and T. O. Yeates, “Verification of protein structures: patterns of nonbonded atomic interactions,” *Protein Sci* 2 (1993): 1511–1519.
 35. J. U. Bowie, R. Lüthy, and D. Eisenberg, “A method to identify protein sequences that fold into a known three-dimensional structure,” *Science* 253 (1991): 164–170.
 36. R. Lüthy, J. U. Bowie, and D. Eisenberg, “Assessment of

- protein models with three-dimensional profiles,," *Nature*, 56 (1992): 83–85.
37. R. A. Laskowski, M. W. MacArthur, D. S. Moss, and J. M. Thornton, "PROCHECK: a program to check the stereochemical quality of protein structures," *J Appl Crystallogr* 26 (1993).
 38. C. J. Williams et al., "MolProbity: More and better reference data for improved all-atom structure validation," *Protein Science* 27 (2018): 293–315.
 39. M. F. Lensink et al., "Blind prediction of homo- and hetero-protein complexes: The CASP13-CAPRI experiment," *Proteins: Structure, Function and Bioinformatics* 87(2019): 1200–1221.
 40. R. Huey and G. M. Morris, "Using AutoDock 4 with ADT: A Tutorial," *Unknown* (2000).
 41. S. Dallakyan and A. J. Olson, "Small-molecule library screening by docking with PyRx,," *Methods Mol Biol* 1263 (2015): 243–250.
 42. N. M. O'Boyle, M. Banck, C. A. James, C. Morley, T. Vandermeersch, and G. R. Hutchison, "Open Babel: An open chemical toolbox," *J Cheminform* 3 (2011): 33.
 43. O. Trott and A. J. Olson, "AutoDock Vina: improving the speed and accuracy of docking with a new scoring function, efficient optimization, and multithreading,," *J Comput Chem* 31 (2010): 455–461.
 44. W. L. Delano, "The PyMOL Molecular Graphics System," *CCP4 Newsletter on protein crystallography* 40 (2002).
 45. S. Rosignoli and A. Paiardini, "Boosting the Full Potential of PyMOL with Structural Biology Plugins," *Biomolecules* 12 (2022): 2022.
 46. E. F. Pettersen et al., "UCSF Chimera--a visualization system for exploratory research and analysis,," *J Comput Chem* 25 (2004): 1605–1612.
 47. A. L. Roman and B. S. Mark, "LigPlot+: Multiple Ligand-Protein Interaction Diagrams for Drug Discovery," *J Chem Inf Model* 51 (2011): 2778–2786.
 48. P. Kesari et al., "Structures of plasmepsin X from *Plasmodium falciparum* reveal a novel inactivation mechanism of the zymogen and molecular basis for binding of inhibitors in mature enzyme," *Protein Science* 31 (2022): 882–899.
 49. B. Mukherjee et al., "Modeling and resistant alleles explain the selectivity of antimalarial compound 49c towards apicomplexan aspartyl proteases," *EMBO J* 37 (2018).
 50. S.P. Leelananda and S. Lindert, "Computational methods in drug discovery," *Beilstein Journal of Organic Chemistry* 12 (2016).
 51. A.V. Sadybekov and V. Katritch, "Computational approaches streamlining drug discovery," *Nature* 616 (2023)-7958.
 52. C.L. Ciana et al., "Novel in vivo active anti-malarials based on a hydroxy-ethyl-amine scaffold," *Bioorg Med Chem Lett* 23 (2013).
 53. L.W. Richardson et al., "Substrate Peptidomimetic Inhibitors of *P. falciparum* Plasmepsin X with Potent Antimalarial Activity," *ChemMedChem* 17 (2022).
 54. V.Kovada et al., "Macrocyclic Peptidomimetic Plasmepsin X Inhibitors with Potent In Vitro and In Vivo Antimalarial Activity," *J Med Chem* 66 (2023): 15.

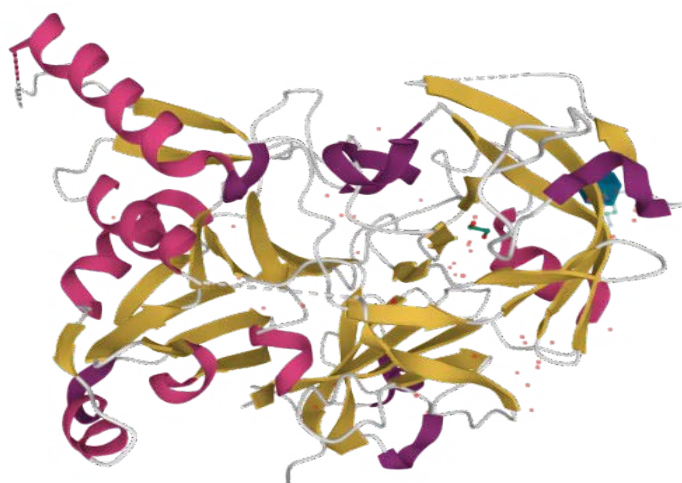


Figure 5: Structure of Plasmepepsin X (PM10, PMX) from *Plasmodium falciparum* 3D7 (PDB code 6ORS). Cartoon representation coloring by secondary structure showing the missing residues in dotted lines. Screenshot from RCSB PDB 3D viewer mol*(javascript) <https://www.rcsb.org/3d-view/6ors>

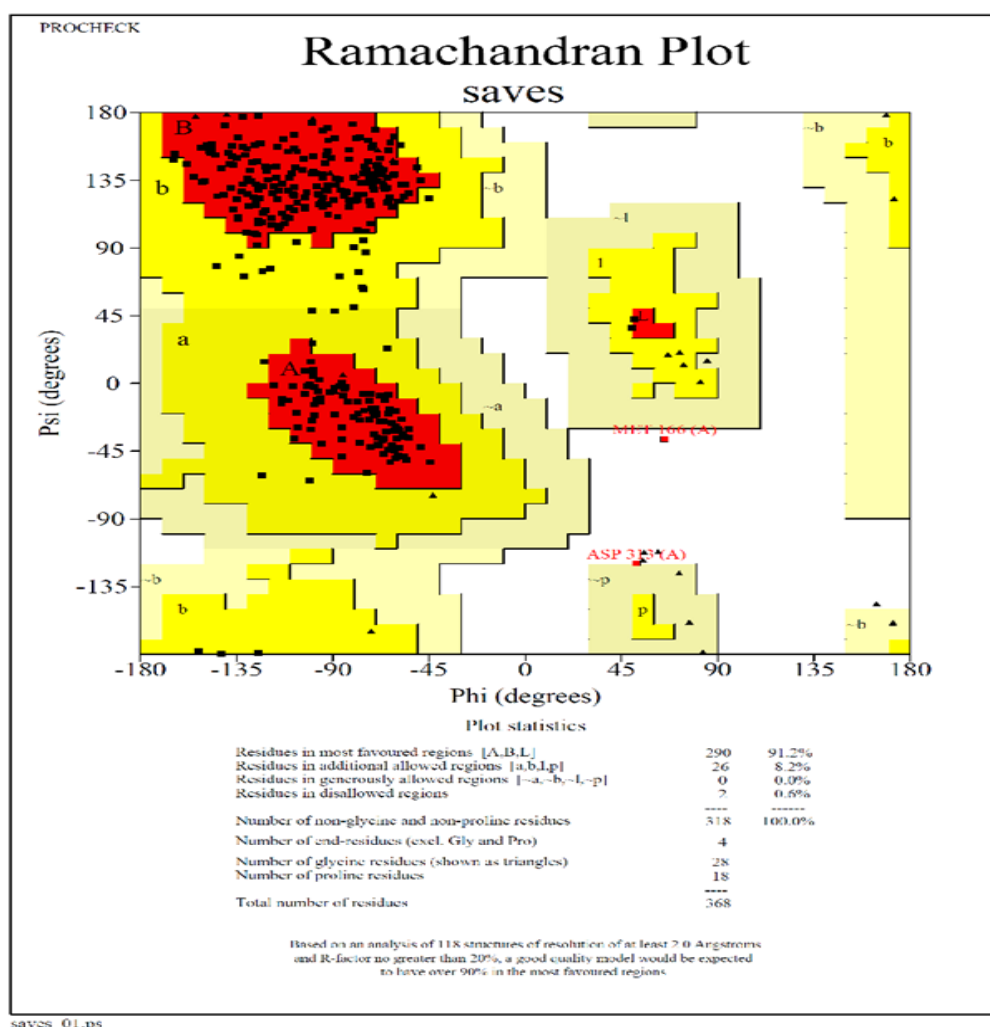


Figure 6: Ramachandran plot of active model of PfPlmX. Residues in most favoured regions are coloured in red, residues in additionally allowed regions in yellow, and residues in generally allowed regions in brown.